nature medicine

Supplementary information

https://doi.org/10.1038/s41591-025-04139-y

Innate antiviral and immune functions associated with the HIV reservoir decay after anti-PD-1 therapy

In the format provided by the authors and unedited

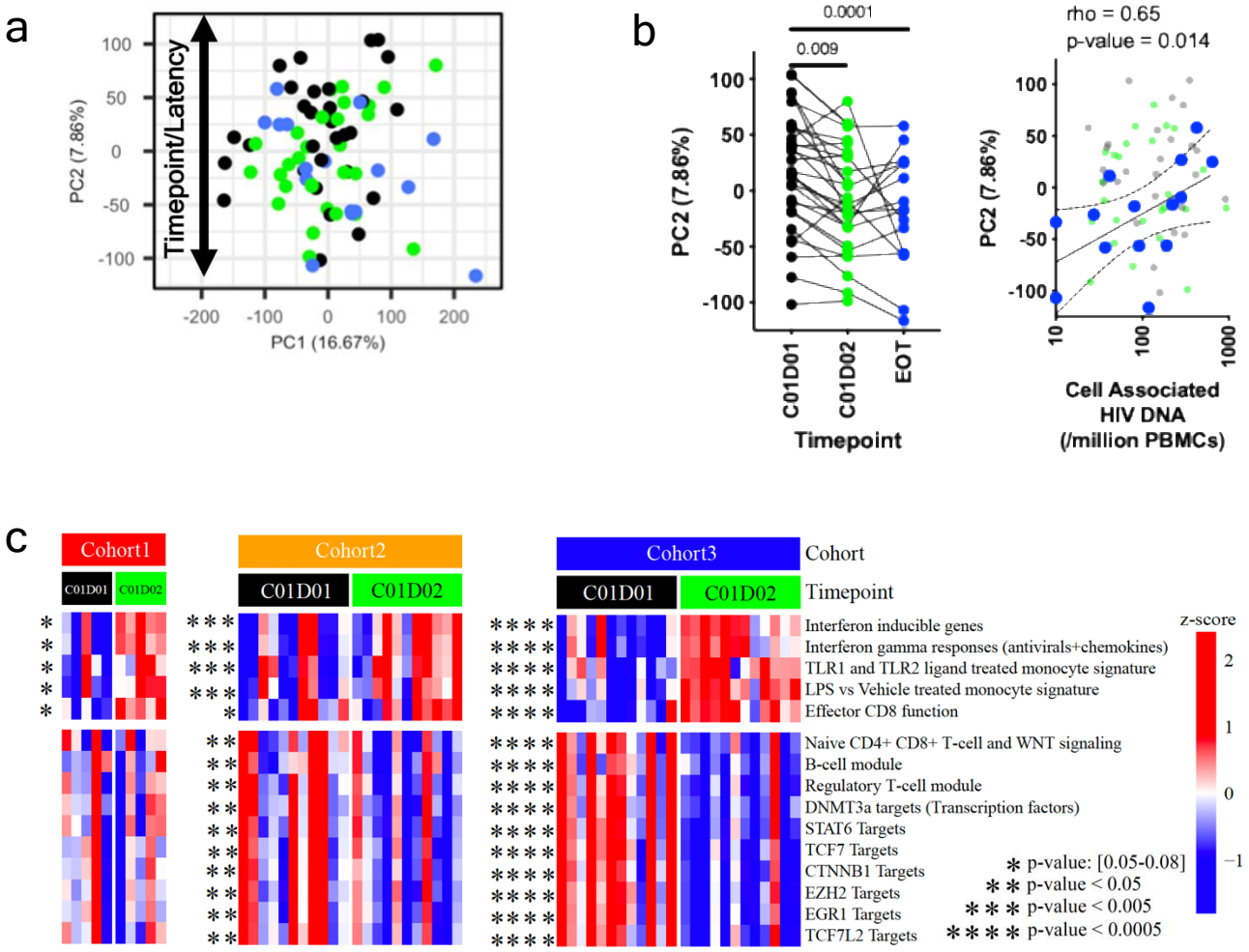

Supplementary Figure 1 | Exploratory analyses of bulk transcriptomic data. (a) Principal component analysis (PCA) of PBMC bulk RNA-seq collected pre-treatment (C01D01, black), 24 h post-treatment (C01D02, green), and at end of treatment (EOT, blue). PC2 captures variance linked to immune activation and temporal proximity to therapy. (b) PC2 scores increased at C01D02 versus baseline (paired two-sided test) (left). PC2 scores at EOT correlated positively with cell-associated HIV DNA. Wilcoxon matched-pairs signed-rank tests assessed changes from C01D01 (right). (c) Sample-level enrichment analysis (SLEA) scores of selected modules across cohorts 1–3 at C01D01 and C01D02. Rows are modules; columns are individuals; color indicates enrichment z-score. Statistical significance is denoted by asterisks: P < 0.05, *P < 0.01, **P < 0.005, ***P < 0.0005.

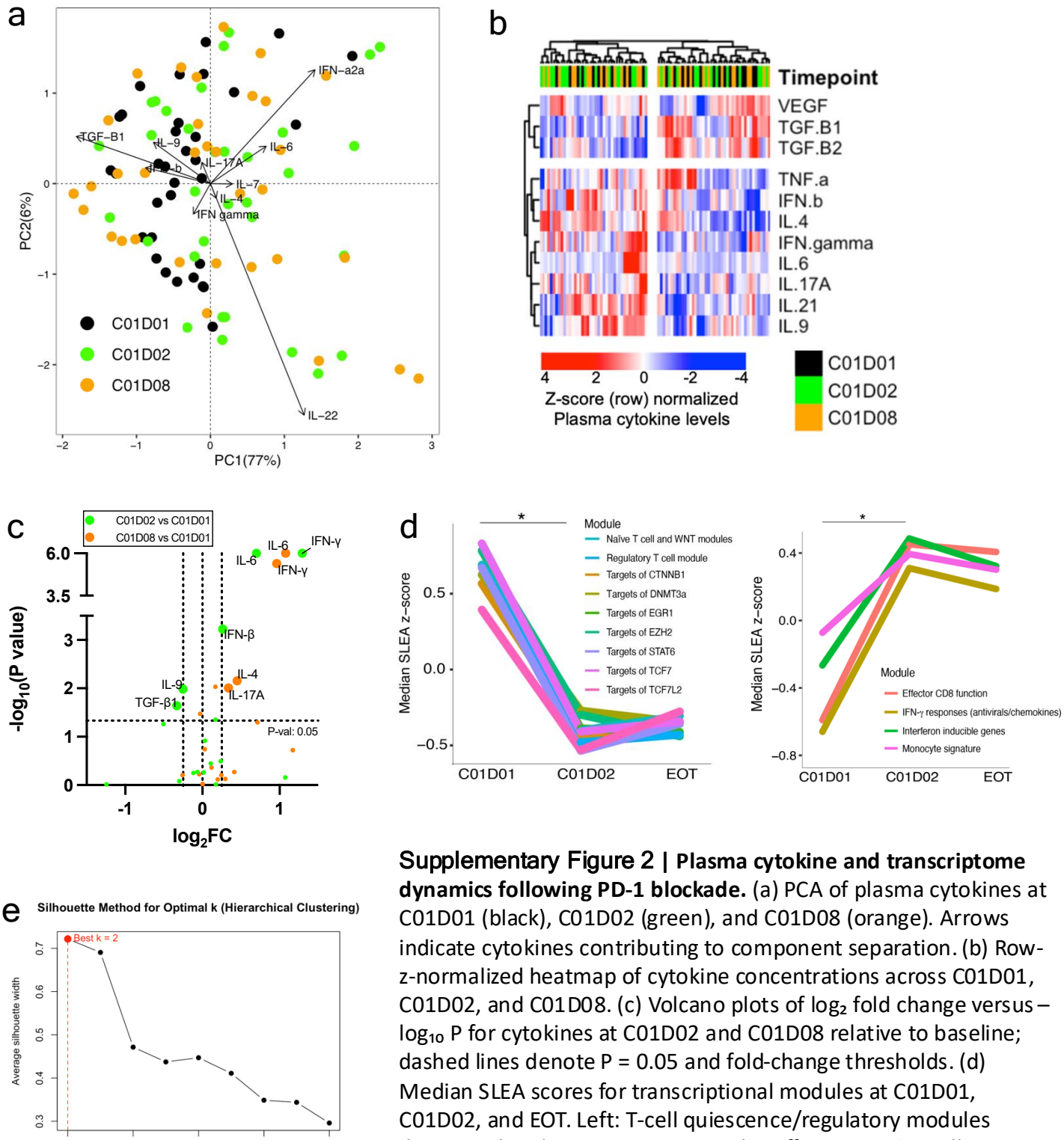

Supplementary Figure 2 | Plasma cytokine and transcriptome dynamics following PD-1 blockade. (a) PCA of plasma cytokines at C01D01 (black), C01D02 (green), and C01D08 (orange). Arrows indicate cytokines contributing to component separation. (b) Row-z-normalized heatmap of cytokine concentrations across C01D01, C01D02, and C01D08. (c) Volcano plots of $\log_2$ fold change versus $-\log_{10}$ P for cytokines at C01D02 and C01D08 relative to baseline; dashed lines denote P = 0.05 and fold-change thresholds. (d) Median SLEA scores for transcriptional modules at C01D01, C01D02, and EOT. Left: T-cell quiescence/regulatory modules downregulated post-treatment. Right: effector $CD8^+$ T-cell, IFN-response, and monocyte-activation modules upregulated by C01D02. (e) Silhouette analysis of hierarchical clustering identifies k = 2 (average silhouette width = 0.71), supporting stratification into Group 1 and Group 2.

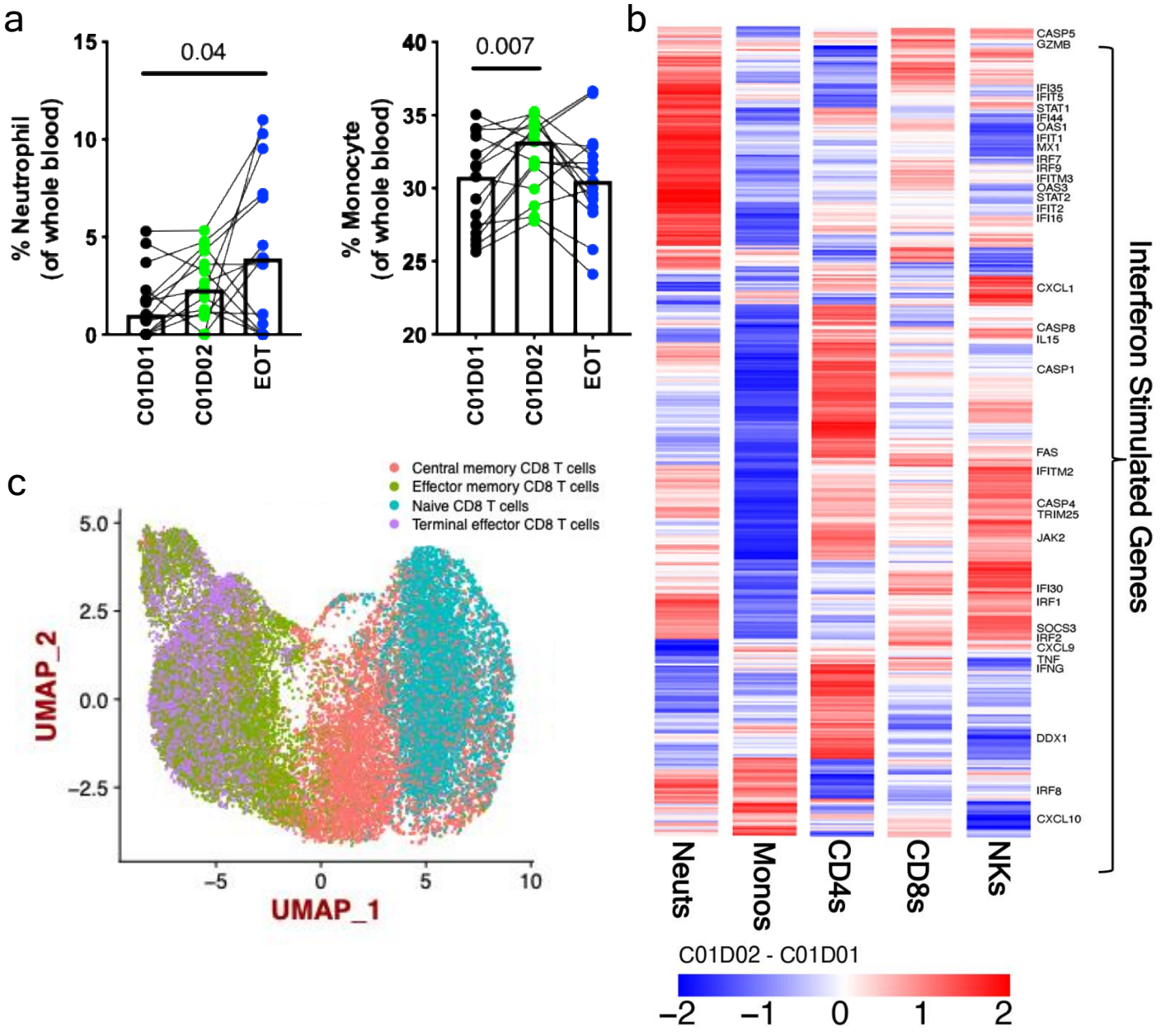

Supplementary Figure 3 | Increase in innate immune cell frequencies and ISG expression after treatment with anti-PD1. (a) CIBERSORT deconvolution of bulk RNA-seq from 15 participants comparing circulating neutrophils and monocytes at C01D01, C01D02, and EOT; paired comparisons to baseline by Wilcoxon matched-pairs signed-rank test. (b) Heatmap of ISG differential expression across immune cell types deconvoluted from bulk RNA-seq by CIBERSORT, comparing C01D02 versus C01D01. (c) UMAP of CD8$^+$ T cells colored by memory subset (naïve, central memory, effector memory, terminal effector).

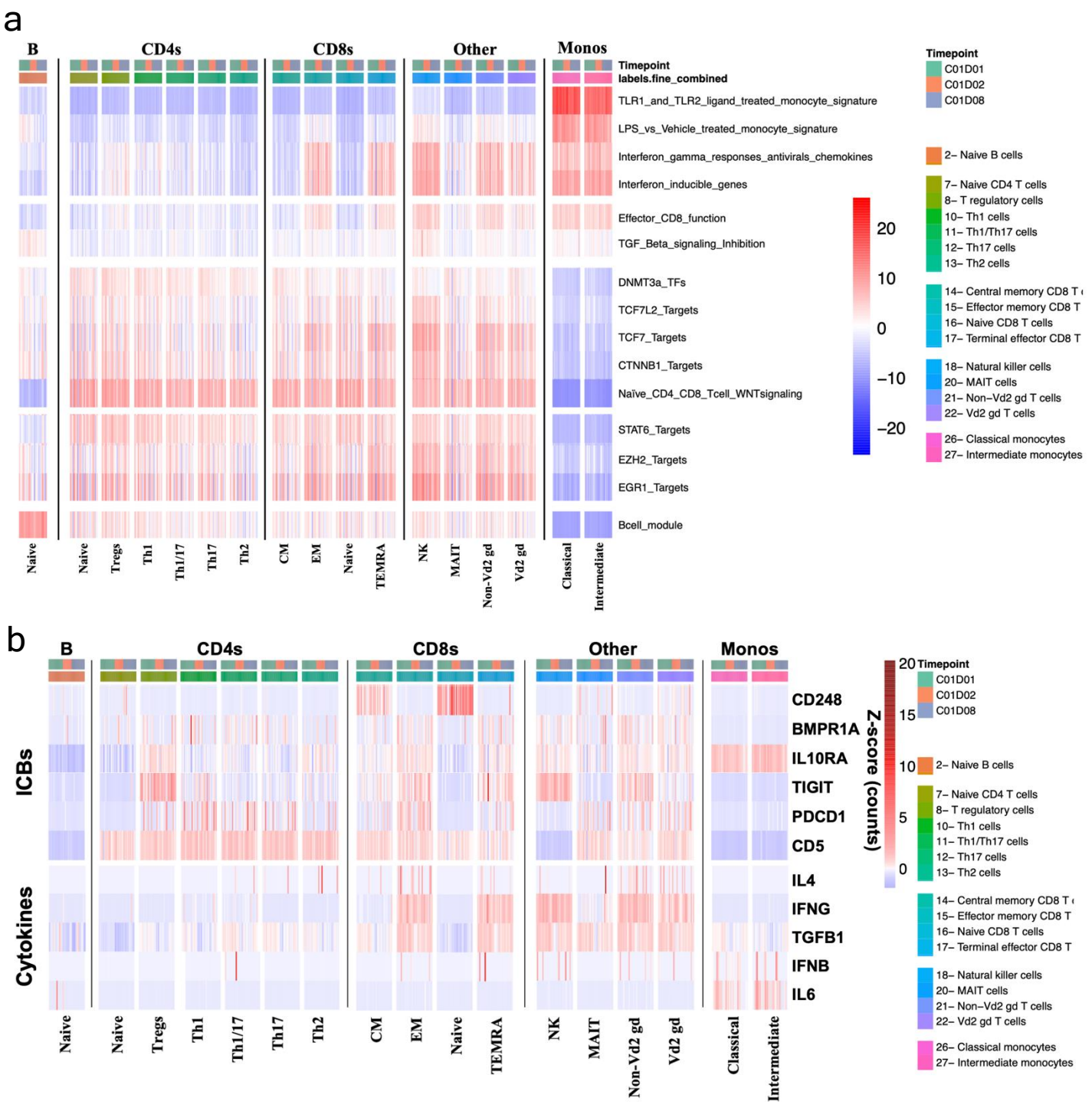

Supplementary Figure 4 | Transcriptomic module, ICB and cytokine expression in key immune cell subsets. (a) Module scores for fine-labeled immune subsets from scRNA-seq (interferon responses, monocyte signatures, exhaustion pathways, TF targets). (b) Expression of selected immune-checkpoint blockade targets and cytokines across annotated subsets.

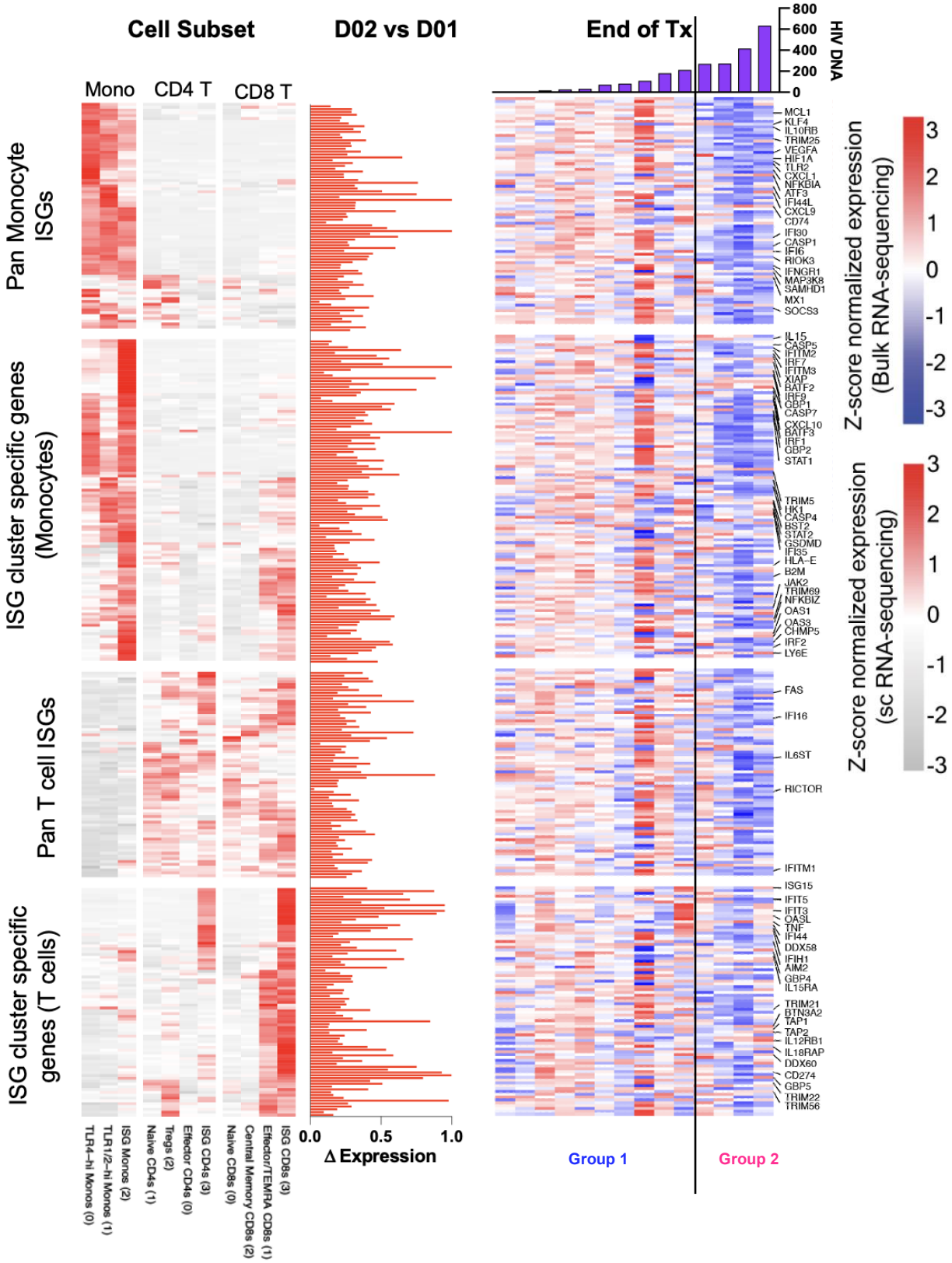

Supplementary Figure 5 | Combined heatmap showing cell subset level expression, change in transcript level with anti-PD1 treatment and viral outcome. Left: differential expression of ISG modules across monocytes, CD4⁺ T cells, and CD8⁺ T cells comparing C01D02 versus C01D01 (pan-ISGs and cluster-specific ISG signatures). Bars show average Δ expression in bulk RNA-seq at 24 h versus pre-treatment. Right: heatmap of EOT ISG expression stratified by HIV-DNA copies per million cells; top bars indicate HIV DNA levels; participants grouped by response (Group 1, blue; Group 2, pink). Representative antiviral/ISG genes are annotated.